Chiang Mai J. Sci. 2008; 35(2) : 274-282
www.science.cmu.ac.th/journal-science/josci.html
Contributed Paper

Effect of Silver Dispersion on Photocatalytic Activity of Silver-Loaded Titanium Oxide

Rungnapa Tongpool* and Kongthip Setwong
National Metal and Materials Technology Center, 114 Paholyothin Rd., Klong Luang, Pathum Thani, 12120, Thailand.
*Author for correspondence; e-mail: rungnapt@mtec.or.th

Received: 3 September 2007
Accepted: 10 October 2007.

ABSTRACT

The improvement of photocatalytic activity of TiO_2 was studied by heat treating the mixtures of silver nitrate solution and three different sizes of TiO_2; commercial-grade C02 (71 nm), P25 (24 nm) and homemade precipitated TiO_2 ($pTiO_2$, 11 nm). The activity toward nitrite degradation of large particles (C02) can be improved to be equal to small particles (P25) by optimum Ag loading. The optimum loading for $pTiO_2$, P25 and C02 were 2.0, 0.75 and 0.75% which corresponded to the Ag contents of 1.35, 0.74 and 0.66%, respectively. Small particles tended to have high, while large particles tended to have low Ag contents as optimum levels. The agglomeration, dispersion and coverage of Ag on each TiO_2 type were different and able to change the activity order. The Ag agglomerates on C02 were large and not well diffused while those on P25 were small and diffused homogeneously. As a result, the critical content (minimum Ag content creating measurable Ag agglomerates) of large TiO_2 particles was relatively low (C02 = 0.66%) compared to that of the small ones (P25 = 1.24%).

Keywords: photocatalysis, silver, particle size, dispersion, agglomeration.

1. INTRODUCTION

Nitrite was considered as a toxic inorganic pollutant in water due to the waste from livestock, agricultural farm, factories of fertilizer and dye. Biological process can change the harmful nitrite to nitrate and nitrogen but it requires a longer time and a higher cost than catalytic decomposition [1]. Nitrite was hardly decomposed under the sunlight and thus photocatalyst is necessary. TiO_2 has been considered as a safe, efficient and economical photocatalyst for organic and inorganic degradation. Dopants including iron[2], silver [3] and rare-earth metal salts [4] have been used to improve the photocatalytic activity of TiO_2. Dopant might be inactivated after long-term use but Zhang and Yu [5] reported that inactivated silver can be reactivated by ambient light illumination. Therefore Ag-doped TiO_2 for outdoor use is promising.

Normally, the smaller the TiO_2 particle, the higher the activity and the higher the cost. If the activity of large particles could be improved to be close to the small ones, the cost for photocatalyst would be saved. However, there was no report on the optimum loading level for various size of TiO_2. There were reports on the suppression of

photocatalytic activity beyond the optimum loading level as a result of separated phases of the oxides of the dopants [2], the reduction of the active sites on photocatalyst [6], the increase of electron-hole pair recombi-nation at the doping sites [7], [8] and at the oxygen vacancies [9]. However, there was no report on the effect of dopant agglomeration and dispersion on photocatalytic activity order. In this paper, three types of TiO_2 were studied; commercial-grade C02, commercial-grade P25 and homemade precipitated TiO_2 ($pTiO_2$). These three powders are different in sizes, crystallinity and surface area. The optimum loading, agglomeration and dispersion of Ag on TiO_2 and their influence on TiO_2 activity were investigated. It was known that crystallinity, particle size and surface area are important factors for photocatalytic activity. In this work, we found that each TiO_2 type was influenced by some factors over the others.

2. MATERIALS AND METHODS

2.1 Materials Preparation

The homemade precipitated TiO_2, denoted as $pTiO_2$, was obtained from hydrolysis reaction of tetraisopropyl orthotitanate ($Ti(OC_3H_7)_4$, Fluka) and calcination at 450°C for 1 h. Commercial-grade TiO_2; P25 (J.J. Degussa) and C02 (Smith supply, Thailand, no. 02), were also used as the undoped samples. The particle sizes of $pTiO_2$, P25 and C02 were 11.1±5.5, 23.9±8.8 and 71.0±23.5 nm, respectively and their surface areas were 126.1±1.1, 54.3±1.5, 11.8±0.4 $m^2 g^{-1}$, respectively. The C02 was in anatase phase and were higher in crystallinity than P25 which was in a mixed phase of anatase and rutile. The $pTiO_2$ was entirely anatase and much lower in crystallinity than C02 and P25.

The Ag-doped precipitated TiO_2, denoted as Ag-$pTiO_2$, was obtained from co-precipitation of $Ti(OC_3H_7)_4$ in $AgNO_3$ (BDH, AnalaR) solution. The Ag-doped P25 and Ag-doped C02, denoted as Ag-P25 and Ag-C02, respectively, were obtained from mixing the respective powder with $AgNO_3$ solution. All the mixtures were stirred for 1 h and then evaporated and calcined at 450°C for 1 h. The atomic ratios of Ag and Ti in the samples were 0.5-3.0%. The doped samples were thoroughly washed before further used.

2.2 Analysis and Characterization

Scanning electron microscope (JSM5410) with INCA 300 energy-dispersive spectrometer (EDS) was used to determine Ag contents in the samples. Transmission electron microscopy (TEM) was carried out with transmission electron microscope (JEOL JEM 1220) using an accelerating of 200 keV. Surface area of the samples was obtained by BET surface area analysis using surface area analyzer (Micromeritics FlowSorb II 2300) and the method followed ISO 9277.

2.3 Photocatalytic Activity

The TiO_2 samples were added to 0.5 ppm $NaNO_2$ aqueous solution (pH = 5.40) in the concentration of 0.001 g ml^{-1}. Before irradiation, the suspensions were stirred for 30 min to ensure equilibration of nitrite over the samples. Then, they were exposed to the UV light of 365 nm (UVP Inc., UVLS 26) for 3, 5, 15 and 30 min in the distance of 25 cm from the UV lamp. The suspensions were stirred all the time. After irradiation, the suspensions were centrifuged and the clear solutions were analyzed by standard *N*-(1-naphthyl) ethylene diamine hydrochloride colorimetric method. The absorbance was measured using UV-Visible spectrometer (JASCO V-530) at 540 nm. Nitrite degradation was determined according to equation (1) [10];

$$n = (c_0-c)/c_0 *100 \quad \text{..... (1)}$$

where n is % conversion, c_0 and c are concentrations of the nitrite solutions before and after irradiation, respectively.

3. RESULTS AND DISCUSSION

3.1 Catalyst Characterisation

The ionic radii of Ag (Ag^+ = 1.26 °A) are larger than those of Ti (Ti^{4+} = 0.68 °A) and thus they stays on the surface of TiO_2 particles. Ag agglomerates were detected when the Ag loadings of Ag-P25 and Ag-C02 were equal or higher than 1.5 and 0.75%, respectively (Figure 1) which corresponded to the Ag contents of 1.24 and 0.66%, respectively (Table 1). The minimum Ag content initiating agglomeration, denoted as a critical content, for C02 was relatively low compared to that for P25 because the first has relatively low surface area for Ag to attach. This can also be seen in 0.75%Ag-P25 (Figure 1a) and 0.75%Ag-C02 (Figure 1d) which had almost equal Ag contents (0.7%) (Table 1) but Ag agglomerates were not seen on the first but clearly seen on the latter. Ag on Ag-pTiO_2 cannot be distinguished by TEM (Figure 1f) but was detected by EDS (Table 1).

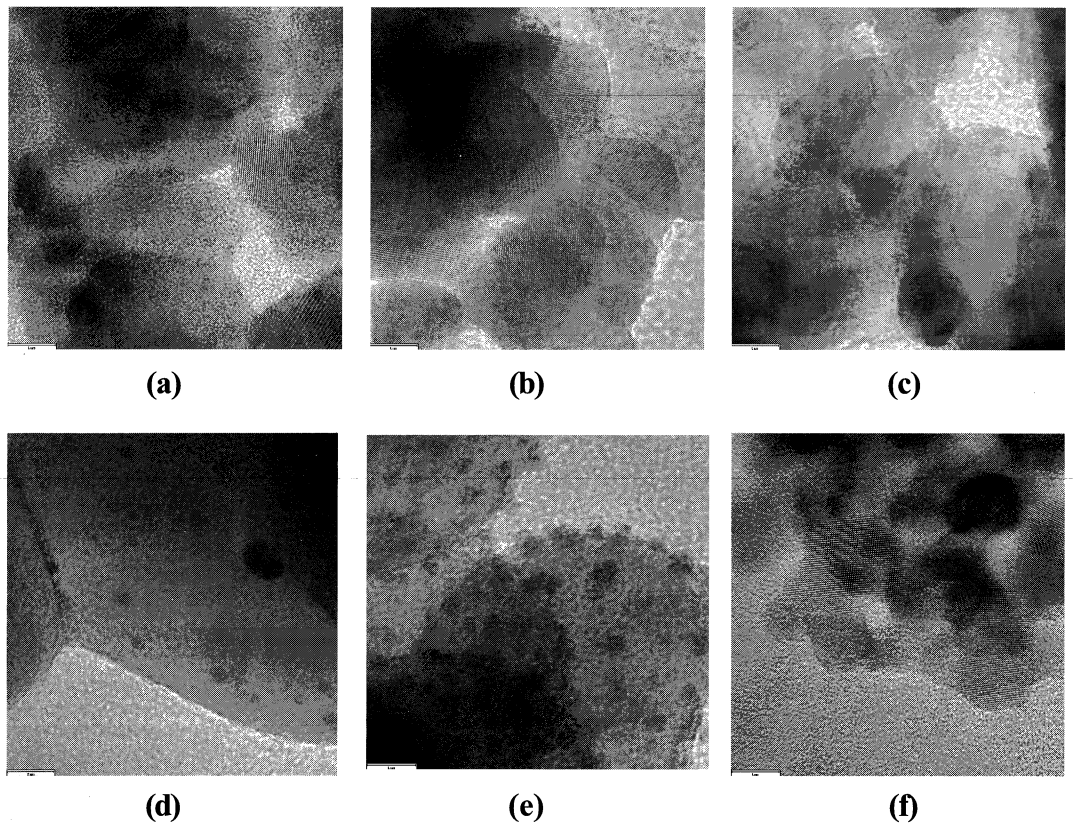

Figure 1. TEM images of the particles of (a) 0.75%Ag-P25, (b) 1.5%Ag-P25, (c) 2.0% Ag-P25, (d) 0.75%Ag-C02 and (e) 2.0%Ag-C02 and (f) 2.0%Ag-pTiO_2. Bars at the bottom left are 8 nm long.

Table 1. Ag contents, atom density indicators (x/y) and Ag agglomerate sizes for the samples that were loaded with various Ag amounts during the doping process.

samples	Ag loading (%)	Ag content (%)	x/y	Ag size (nm)
Ag-pTiO$_2$	1.5	1.28	0.012	no*
	2.0	**1.35**	0.013	no
	2.5	1.79	0.017	no
	3.0	2.76	0.026	no
Ag-P25	0.5	0.47	0.008	no
	0.75	**0.74**	0.013	no
	1	0.90	0.016	no
	1.5	1.24	0.025	small**
	2	1.83	0.035	2.9
Ag-C02	0.5	0.50	0.026	no
	0.75	**0.66**	0.034	2.9
	1	0.85	0.044	4.7
	1.5	1.05	0.050	3.6
	2	1.27	0.068	4.0

* no : cannot be seen or distinguished

** small : too small to be measured

If the Ag content, x, is divided by the surface area, y m^2 g^{-1}, the obtained value, x/y, is proportional to the number of Ag atoms per unit surface area, denoted as atom density indicator, according to equations (2)-(4). The atom density indicators (x/y) of the Ag-doped samples were shown in Table 1.

TiO$_2$ is consisted of Ti = (6.02 x 10^{23} atoms mole^{-1})/(79.9 g mole^{-1})
= 7.53 x 10^{21} atoms g^{-1} .....(2)

Ag atoms per unit surface area
= (x Ag atoms/100 Ti atoms) x ($1/y$ m^2 g^{-1}) x (7.53 x 10^{21} Ti atoms g^{-1})
.....(3)

= (x/y) x 7.53 x 10^{19} Ag atoms m^{-2}
.....(4)

At high Ag loading, the Ag contents detected in Ag-C02 were lower than those detected on Ag-P25 and Ag-pTiO$_2$. A distinct explanation goes to the low surface area of C02, having few reaction sites for Ag to react with. However, the atom density indicator in Table 1 shows that, for the same Ag loading, the Ag density on Ag-C02 was the highest. This means that the Ag dispersion on C02, P25 and pTiO$_2$ were not the same. In one unit area, C02 carried Ag atoms more than P25 and pTiO$_2$ did. However, TEM images show that, Ag agglomerates on Ag-C02 were far apart from one another unlike what to be expected from their high atom density indicators. We found that the size of Ag agglomeration on Ag-C02 were relatively large as (Table 1). This leads to the conclusion that the Ag on Ag-C02 tended to form large agglomerates and did not disperse well. This is clearly seen in 0.75%Ag-C02 (Figure 1d) and 2.0%Ag-P25 (Figure 1c), having the same atom density indicators of 0.034-0.035, that Ag agglomerates on the first were far apart from one another while those on latter were close to one another (Figure 1).

Absorption of the nitrite solution on the photocatalyst would influence the photocatalytic activity. However we did not find the absorption of 0.5 and 1 ppm nitrite solutions on the TiO_2 samples.

3.2 Photocatalytic Activity Measurement

Without TiO_2 sample, nitrite solution was not degraded although it was under 2-h UV exposure. This is because the bond strength within a nitrite molecule is too high to be broken by the energy of 365-nm UV light. With P25 and the Ag-doped samples, nitrite degradation of 100% can be achieved under 30-min UV exposure (Figure 2). P25 showed much higher photocatalytic activity than C02 and $pTiO_2$ but after Ag loading, the activities of C02 and $pTiO_2$ were tremendously increased (Figure 3 and 4) while the activity of P25 was slightly increased.

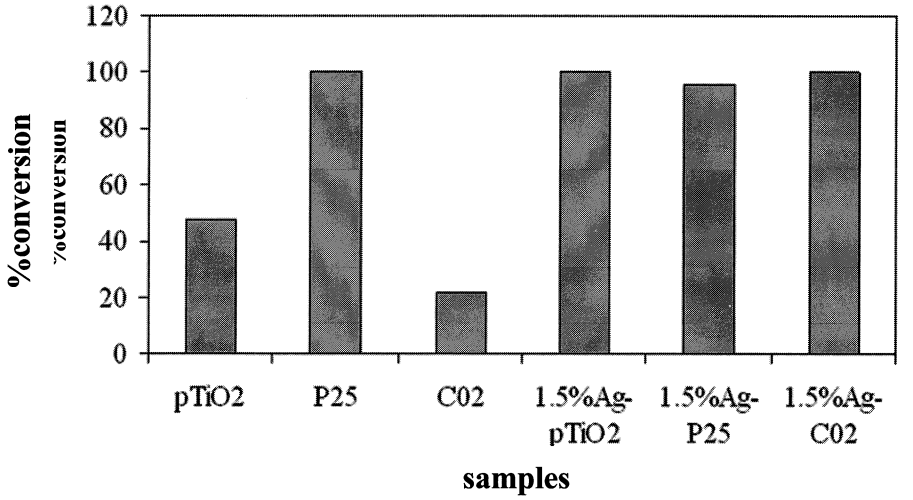

Figure 2. shows % conversion of nitrite with TiO_2 samples after 30-min UV exposure.

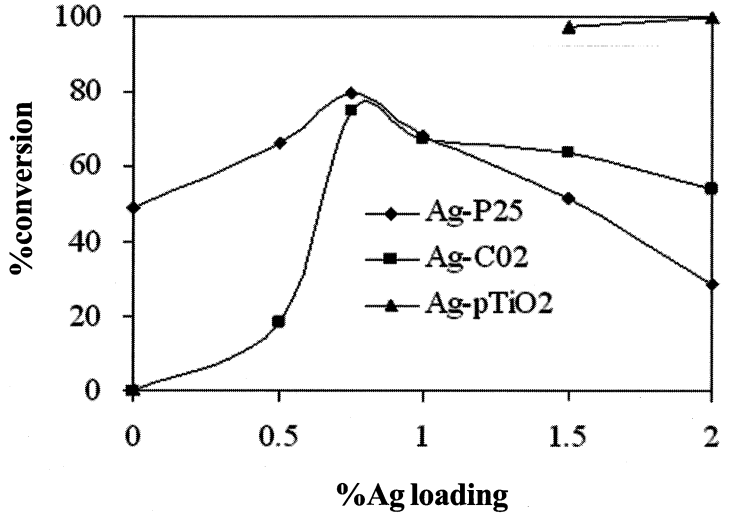

Figure 3. shows effect of Ag loading on photocatalytic activities of P25, C02 and $pTiO_2$ under 5-min UV exposure.

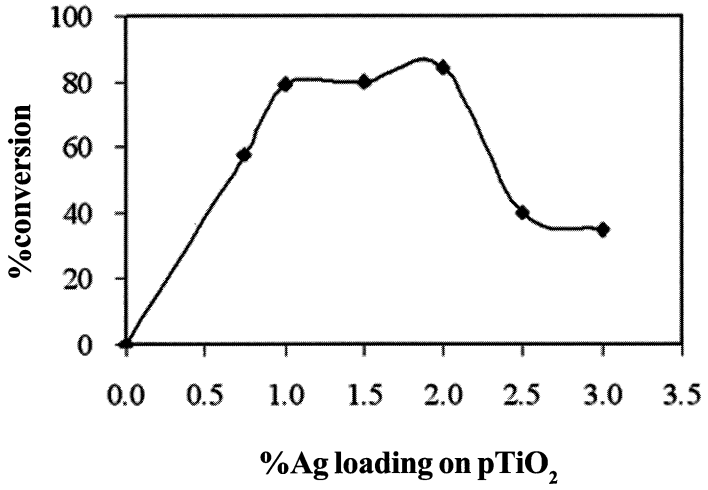

Figure 4. shows effect of Ag loading on photocatalytic activities of $pTiO_2$ after 3-min UV exposure.

Figure 3 shows the effect of Ag loading on nitrite degradation after 5-min UV exposure. The optimum loading levels for both Ag-P25 and Ag-C02 were 0.75% which corresponded to the Ag contents of 0.74 and 0.66%, respectively (Table 1). The highest activities of Ag-P25 and Ag-C02 were nearly the same although the surface area of the first was about three times of the latter. Below the optimum loading level, the activities of Ag-P25 were higher than those of Ag-C02 but beyond the optimum loading level, the activities of the first were lower than the latter. Ag-$pTiO_2$ showed the highest activities and the optimum loading level was distinguished by 3-min UV exposure shown in Figure 4. The Ag loadings of 1.0, 1.5 and 2.0% showed very high activities and the highest was achieved at 2.0 % which corresponded to the Ag content of 1.35 %.

Figure 5 shows the time courses of nitrite degradation up to 15 min irradiation on the selected samples. It can be seen that Ag-$pTiO_2$ presented the highest initial rate and 80 % conversion could be achieved after 3 min. 0.75%Ag-P25 was slightly faster than 0.75%Ag-C02 and 75 % conversion could be achieved within 5 min. The undoped samples showed relatively low degradation rates.

For all reactions, there are three important factors determining reaction rate; (i) reactant concentration, (ii) number of reaction sites and (iii) activation energy. For photocatalytic reactions, reactants include materials to be degraded, photogenerated hole (h^+) and electron (e^-), adsorbed water, hydroxide, oxygen and hydroxyl radical ($^{\bullet}OH$). Reaction sites include the surface area of the photocatalyst and the interface between the photocatalyst and materials to be degraded. Activation energy includes photon flux reaching the photocatalyst, generating excited h^+, e^-, $^{\bullet}OH$ and degradation products.

P25 was more active than $pTiO_2$ although the first was about half in the surface area of the latter. This is because $pTiO_2$ was low in crystallity and thus photogenerated charges were recombined before and after reaching the surface, leaving few photogenerated holes and electrons to react with adsorbed water

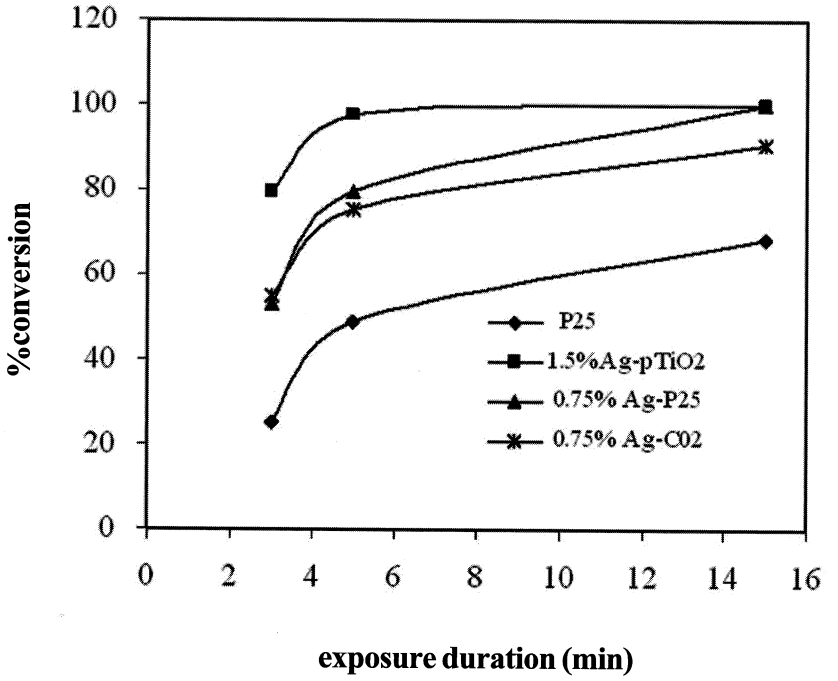

Figure 5. shows %nitrite conversion vs. UV exposure duration of the undoped and doped samples.

and hydroxide to produce hydroxyl radical (equations (5)-(8), [2, 10, 11]. These hydroxyl radicals are needed to oxidize nitrite molecules [2, 4] (equation (9)). Even though the number of reaction sites on $pTiO_2$ was high, the number of charges for reaction to take place was small.

$2h^+ + 2H_2O \rightarrow 2\ ^\bullet OH + 2H^+$ .....(5)

$2h^+ + 2OH^- \rightarrow 2\ ^\bullet OH$ .....(6)

$e^- + O_2 \rightarrow O_2^{\bullet-}$ .....(7)

$2O_2^{\bullet} + 2H_2O \rightarrow 2\ ^\bullet OH + 2OH^- + O_2$ .....(8)

$NO_2^- + 2\ ^\bullet OH \rightarrow NO_3^- + H_2O$.....(9)

P25 was higher in photocatalytic activity than C02. The first was lower in crystallinity but higher in surface area than the latter. Since P25 was well crystalline compared to $pTiO_2$, the charge recombination was relatively small. There were a number of charges reached the reaction sites and thus having high surface area was useful in this case.

The Ag-doped samples performed much better than the undoped samples. As Ag has higher work function than TiO_2, it attracts photogenerated electrons arriving at the particle surface [7, 12] leaving a large number of holes for further reactions. Pleskov [13] and Xu, et al [4] reported that, to achieve good charge separation, the value of space charge region potential must be not lower than 0.2 V. For small colloidal particles, there is nearly no band bending and the space charge region potential is low. Dopant is needed to increase the space charge region potential. However, as the concen-tration of dopant ions increases, the space charge region becomes narrower. If the penetration depth of light into TiO_2 exceeds the space charge layer, charge recombination becomes easier. Therefore the dopant amount should be high enough to induce the potential but low enough to obtain wide layer of space charge region.

Apart from the good charge separation, we found that the behaviour of Ag agglomeration, dispersion and coverage on each type of TiO_2 played important role on determination of their optimum loading levels. It was shown in Figure 3 that below the optimum loading level, Ag-C02 performed much worse than Ag-P25 but beyond the optimum loading level, Ag-C02 performed better than Ag-P25 although the first was much lower in surface area than the latter. It was seen in Figure 1 that the Ag agglomerates on 2.0%Ag-P25 were closed to one another and covered a large area of the particle surface while those on 2.0%Ag-C02 were relatively far apart from one another and covered a relatively small area of the particle surface. They tended to form large agglomerates instead of spreading onto the C02 surface. Although the size of Ag agglomerates on 1.0 and 1.5%Ag-P25 cannot be measured by HRTEM, it could be postulated that large portions of their surface area were covered with tiny Ag agglomerates. The coverage of Ag agglomerates can (i) block light from reaching the reaction sites (called a filter effect [1], (ii) reduce the number of reaction sites on TiO_2 surface [6], (iii) become defects and charge recombination sites [5, 7] and thus reduce photocatalytic activity.

Each TiO_2 type had its own optimum loading level, depending on the behaviour of the agglomeration, dispersion and coverage of the Ag on each TiO_2 type. This behaviour affect photogenerated charge separation, the number of reaction sites and the photon flux. Small particles tend to have high, while large particles tend to have low Ag contents as optimum loading levels.

4. CONCLUSIONS

The activity of large TiO_2 particles can be improved by optimum Ag loading. The optimum loading level was influenced by the particle size and surface area of TiO_2 and the dispersion and agglomeration of Ag on TiO_2 particles. This is to obtain a good charge separation, maximum photon flux and maximum reaction sites. The optimum loading level for Ag-pTiO_2, Ag-P25 and Ag-C02 were 2.0, 0.75 and 0.75%, respectively, which corresponded to the Ag contents of 1.35, 0.74 and 0.66%, respectively. Small particles tended to have high, while large particles tended to have low Ag contents as optimum loading levels. The agglomeration and dispersion of Ag on the three kinds of TiO_2 were different. The Ag on C02 tended to form large agglomerates and did not disperse well while the Ag on P25 formed relatively small agglomerates and diffused homogeneously. This is why the critical content (minimum Ag content creating measurable Ag agglomerates) of C02 was relatively low (0.66%) compared to that of P25 (1.24%).

ACKNOWLEDGEMENTS

This work was supported by National Metal and Materials Technology Centre, Thailand. We acknowledge our colleagues for the help on characterization techniques.

REFERENCES

[1] Nemoto J., Gokan N., Ueno H. and Kaneko M., Photodecomposition of ammonia to dinitrogen and dihydrogen on platinized TiO_2 nanoparticules in an aqueous solution, J. Photochem. Photobiol. A, 2007; 185: 295-300.

[2] Navío J., Colón A., Trillas M., Peral J., Domènech X., Testa J. J., Padrón J., Rodríguez D. and Litter M.I., Heterogeneous photocatalytic reactions of nitrite oxidation and Cr(VI) reduction on iron-doped titania prepared by the wet impregnation method, Appl. Catal., B 1998; 16: 187-196.

[3] Chang C.-C., Lin C.-K., Chan C.-C., Hsu C.-S. and Chen C.-Y., Photocatalytic properties of nanocrystalline TiO_2 thin film with Ag addition, Thin Solid Films, 2006; 494: 274-278.

[4] Xu A.-W., Gao Y. and Liu H.-Q., The preparation, characterization, and their photocatalytic activities of rare-earth-doped TiO_2 nanoparticles, J. Catal., 2002; 207: 151-157.

[5] Zhang L. and Yu J.C., A simple approach to reactivate silver-coated titanium dioxide photocatalyst, Catal. Commun., 2005; 6: 684-687.

[6] Domenech X. and Peral J., Kinetics of the photocatalytic oxidation of N(III) and S(IV) on different semiconductor oxides, Chemosphere, 1999; 38: 1265-1271.

[7] Zhang L., Yu C., Yip H.Y., Li Q., Kwong K.W., Xu A.-W. and Wong P.K., Ambient light reduction strategy to synthesize silver nanoparticles and silver-coated TiO_2 with enhanced photocatalytic and bactericidal activities, Langmuir, 2003; 19: 10372-10380.

[8] Zhang F., Jin R., Chen J.C., Shao C., Gao W., Li L. and Guan N., High photocatalytic activity and selectivity for nitrogen in nitrate reduction on Ag/TiO_2 catalyst with fine silver clusters, J. Catal., 2005; 232: 424-43.

[9] Irie H., Watanabe Y. and Hashimoto K., Nitrogen-concentration dependence on photocatalytic activity of $TiO_{2-x}N_x$ powders, J. Phys. Chem. B 2003; 107: 5483-5486.

[10] Shifu C. and Gengyu C., Photocatalytic oxidation of nitrite by sunlight using TiO_2 supported on hollow glass microbeads, Solar Energy, 2002; 73: 15-21.

[11] Ireland J.C., Klostermann P., Rice E.W. and Clark R.M., Inactivation of Escherichia Coli by titanium dioxide photocatalytic oxidation, Appl. Environ. Microbiol., 1993; 59: 1668-1670.

[12] Yang P., Lu C., Hua N. and Du Y., Titanium dioxide nanoparticles co-doped with Fe^{3+} and Eu^{3+} ions for photocatalysis, Mater. Lett., 2002; 57: 794-801.

[13] Pleskov Y.V., Conversion of luminous energy into electrical and chemical energy in photoelectrochemical cells with semiconductor electrodes, Sov. Electrochem., 1981; 17: 1-25.